

# Virtual Screening, Toxicity Evaluation and Pharmacokinetics of Erythrina Alkaloids as Acetylcholinesterase Inhibitor Candidates from Natural Products

Afri Permana<sup>1</sup>, Abd Wahid Rizaldi Akili<sup>1</sup>, Ari Hardianto<sup>1</sup>, Jalifah Binti Latip<sup>2</sup>, Allyn Pramudya Sulaeman<sup>1</sup>, Tati Herlina<sup>1</sup>

<sup>1</sup>Department of Chemistry, Faculty of Mathematics and Natural Science, Universitas Padjadjaran, Sumedang, West Java, Indonesia; <sup>2</sup>Department of Chemical Sciences, Faculty of Science and Technology, Universiti Kebangsaan Malaysia (UKM), Selangor, Malaysia

Correspondence: Tati Herlina, Email [tati.herlina@unpad.ac.id](mailto:tati.herlina@unpad.ac.id)

**Purpose:** Alzheimer's disease (AD) is a progressive neurodegenerative disorder with limited treatment options, necessitating the development of safer and more effective therapies. The potential of alkaloids derived from the genus *Erythrina* as acetylcholinesterase (AChE) inhibitors is being investigated to enhance acetylcholine levels in the brain, which is crucial for the treatment of AD. The objective of this study is to identify Erythrina alkaloids with strong inhibitory capacity against AChE and favorable pharmacokinetic profiles.

**Materials and Methods:** A multi-step computational approach was employed, beginning with the virtual screening of 143 Erythrina alkaloid structures using molecular docking against the human AChE crystal structure. The binding affinities were compared with the known AChE inhibitor, galantamine. The top alkaloid, 8-oxoerythrinanthine (**128**), was subjected to further analysis through molecular dynamics simulations, with the objective of evaluating its stability and interactions. In silico ADMET predictions were conducted to assess the pharmacokinetic properties. The applicability of Lipinski's Rule of Five was applied to evaluate oral drug-likeness.

**Results:** 8-Oxoerythrinanthine (**128**) exhibited the highest binding affinity and remarkable stability in molecular dynamics simulations. The toxicity predictions indicated a low risk of mutagenicity, hepatotoxicity, and cardiotoxicity. Pharmacokinetic assessments indicated good absorption, moderate blood-brain barrier penetration, and favorable metabolic and excretion profiles, supporting its potential as an orally active drug candidate.

**Conclusion:** 8-Oxoerythrinanthine (**128**) exhibits strong potential as an AChE inhibitor with a favorable balance of efficacy, safety, and pharmacokinetic properties. These results warrant further investigation in preclinical and clinical studies to validate its therapeutic potential and safety for Alzheimer's disease treatment.

**Keywords:** Erythrina alkaloid, pharmacokinetics, In silico, acetylcholinesterase inhibitors, virtual screening

## Introduction

Alzheimer's disease (AD) is a chronic neurodegenerative disorder characterized by protein-conformational disease (PCD) resulting from aberrant processing of protein and polymerization. When soluble neuronal proteins fail to fold (due to genetic mutations, environmental conditions, or aging), they assemble, leading to aberrant neuronal function and loss.<sup>1</sup> Alzheimer's disease is the leading cause of progressive dementia, characterized by significant cognitive decline and a major impact on an individual's independence and orientation. According to estimates by Alzheimer's Disease International (ADI), around 75% of individuals with dementia remain undiagnosed. In several low- and middle-income countries, the percentage reaches 90%.<sup>2,3</sup> As stated by the World Health Organization (WHO), Alzheimer's disease represents a significant global public health concern, accounting for 60–70% of all dementia cases.<sup>1</sup> Alzheimer's

is a chronic neurological disease and a form of dementia that affects over 50 million individuals worldwide.<sup>4,5</sup> Without the development of an effective treatment, estimates suggest that this number will rise to 152 million by 2050.<sup>1,6,7</sup>

The number of reported cases of AD worldwide is approximately 24 million, with projections indicating that the number of patients with dementia will quadruple by 2050.<sup>6</sup> There are several hypotheses that have been developed by scientists that explain some of the reasons for the onset and progression of AD, one of which is the cholinergic hypothesis.<sup>8</sup> Proposed over two decades ago, the cholinergic hypothesis posits that neurons in the brain holding acetylcholine have a substantial role in the cognitive decline observed in individuals with advanced age and AD. This idea has been the basis for most treatment approaches and the development of AD treatments.<sup>9</sup> There are several hypotheses that have been developed by scientists that explain some of the reasons for the onset and progression of AD, one of which is the cholinergic hypothesis.

The cholinergic theory has advanced AD research by shifting it from descriptive neuropathology to modern ideas about synaptic neurotransmission. This hypothesis received convincing validation when cholinesterase inhibitor therapy was shown to cause significant improvement in symptoms in patients with AD. Despite the focus in recent years on understanding the diverse pathophysiological pathways of AD, therapies that restore cholinergic function remain an important aspect in the treatment of AD patients.<sup>10</sup> Despite the significant impact of AD on public health, there are presently just two categories of medications authorized for the treatment of this condition: cholinesterase enzyme inhibitors obtained from natural, synthetic, or a combination of both origins, and N-methyl d-aspartate (NMDA) antagonists.<sup>6</sup> The Food and Drug Administration (FDA) has granted approval for the use of two drugs, donepezil and rivastigmine, for the treatment of Alzheimer's disease. However, both have a number of side effects, including nausea, diarrhea, anorexia, fainting, abdominal discomfort, and vomiting. Researchers are therefore looking for new, effective drugs that may provide higher efficacy than existing treatments, but have far fewer negative effects.

The search of chemical compounds derived from natural sources as potential to find potential sources of new drugs is very necessary and needs to be developed along with the increasing need for drugs in the world. The discovery of natural chemical compounds from plants has received more attention, because it provides better side effects and treatment effectiveness. The use of plants as a source of natural chemical compounds is becoming increasingly prevalent due to their reduced incidence of adverse effects and enhanced efficacy in treatment. The diminished propensity for side effects and enhanced biological safety of plant-derived compounds make them a safer alternative to synthetic drugs.<sup>11,12</sup> Natural resources have also been targeted by scientists as prospective anti-AChE drugs, as natural ingredients are usually less harmful than synthetic compounds. Galantamine is a natural drug extracted from the *Galanthus woronowii* plant that is currently used in the treatment of AD along with other chemical drugs approved by the FDA. However, since none of these drugs have proven to be fully effective in halting the development or progression of Alzheimer's disease, research is underway to identify new molecules from natural sources that have anti-AChE properties.<sup>8</sup>

Several AChE inhibitors have been extracted from diverse natural sources. Based on their intricate nitrogen-containing structure, alkaloids are regarded as the most promising options for the therapy of Alzheimer's disease among these natural products.<sup>13</sup> The active site of AChE contains two main subsites, the "esteratic" and "anionic" subsites, which correspond to the catalytic machinery and the choline-binding pocket, respectively. The "esteratic" subsite consists of a histidine residue (HIE447), while the "anionic" subsite is a tryptophan residue (TRP84) capable of binding quaternary ligands, which can act as a competitive inhibitor.<sup>14</sup>

Acetylcholinesterase (AChE) inhibitors are crucial in the management of neurodegenerative disorders, including Alzheimer's disease (AD), by regulating acetylcholine (ACh) concentrations in the synaptic cleft. AChE inhibitors operate at the molecular level by binding to the enzyme's active site, therefore obstructing the hydrolysis of ACh, essential for cholinergic neurotransmission. The catalytic triad of acetylcholinesterase, comprising serine (SER203), glutamate (GLU334), and histidine (HIE447), is essential for its enzymatic function. Inhibition transpires when these chemicals occupy the active site, so obstructing ACh from binding and undergoing hydrolysis.<sup>15,16</sup> The inhibitory mechanism can be categorized into reversible and irreversible forms. Reversible inhibitors, like galantamine, compete with acetylcholine for binding at the active site, whereas irreversible inhibitors establish covalent bonds with the enzyme, resulting in permanent inactivation.<sup>17,18</sup> Moreover, AChE inhibitors may interact with the peripheral anionic site (PAS) of the enzyme, separate from the active site. This contact may influence the enzyme's conformation and potentially diminish

the aggregation of amyloid-beta (A $\beta$ ) peptides, a characteristic of Alzheimer's disease pathogenesis. Compounds that target both the active site and the peripheral anionic site (PAS) are being investigated for their dual role in inhibiting AChE and diminishing A $\beta$  aggregation.<sup>19,20</sup>

Alkaloid compounds from the genus *Erythrina* have the potential as inhibitors of the enzyme AChE which is useful in breaking down acetylcholine into choline and acetate in the decline in thinking and memory of Alzheimer's patients. The decline is caused by a decrease in acetylcholine (ACh) resulting in a loss of presynaptic cholinergic transmission levels. Isolation from plants of the genus *Erythrina* produced alkaloids with erythrinan, 16-azoerythrinan, tetrahydroisoquinoline, benzyloisoquinoline, quinolizidine, indole and dimer skeletons.<sup>13</sup> Generally, plants rich in alkaloids, such as the genus *Erythrina*, contain more than 130 species of alkaloid types.<sup>21</sup> A study examining the anticholinesterase activity of leaf extracts from *Erythrina velutina* found that aqueous extracts are alkaloid-rich extracts can inhibit AChE activity depending on the concentration.<sup>22</sup>

A different study showed that the chloroform fraction of *Erythrina variegata* bark has AChE inhibitory potential with IC<sub>50</sub> values of  $38.03 \pm 1.987$   $\mu$ g/mL for AChE and  $20.67 \pm 2.794$   $\mu$ g/mL. The researchers have established that bioactive compounds containing indole [7a,1-a] isoquinoline functional groups significantly inhibit AChE. Since bioactive compounds with indole [7a,1-a] isoquinoline groups have been documented and recorded for their inhibitory effects against AChE, the six major alkaloids of this species were subjected to molecular inhibition and molecular dynamics simulations to predict the inhibitory potential against AChE. Results indicated that Erysotine and Erythraline alkaloids have the highest binding affinity with AChE. The results of this study provide sufficient evidence supporting the utilization of indole [7a,1-a] isoquinoline derivatives for the identification of new drug molecules in the treatment of AD.<sup>23</sup> To date, there are more than 143 alkaloids that have been isolated from genus *Erythrina*.<sup>21</sup> However, only a few have been investigated for their potential in inhibiting AChE, so further research is needed to screen the potential of *Erythrina* alkaloids as AChE inhibitors.

The exploration of *Erythrina* alkaloids as a potential therapy for Alzheimer's disease (AD) offers a significant opportunity for therapeutic intervention, especially in comparison to current treatments. *Erythrina* alkaloids exhibit mechanisms that may ameliorate cognitive deficits linked to Alzheimer's disease, paralleling the effects of contemporary cholinesterase inhibitors like galantamine, which enhance cholinergic function by preventing the degradation of acetylcholine. Recent research has emphasized the neuroprotective properties of *Erythrina* alkaloids against oxidative stress and neuroinflammation, both of which contribute to the pathogenesis of Alzheimer's disease.<sup>24</sup> *Erythrina* alkaloids provide a favorable safety profile, with studies demonstrating that these compounds do not impair motor activity at effective dosages.<sup>24,25</sup> *Erythrina* alkaloids provide the potential to deliver therapeutic benefits with minimal side effects, making them a compelling alternative or complement to current Alzheimer's disease treatments.

Studies indicate that some *Erythrina* alkaloids possess neuroprotective characteristics, potentially advantageous in the context of Alzheimer's disease. This fosters novel therapeutic approaches for neurodegenerative diseases and has demonstrated a reduction in oxidative parameters in experimental models, suggesting a possible avenue to mitigate cognitive loss associated with Alzheimer's disease.<sup>26</sup> The neuroprotective properties of *Erythrina* alkaloids are associated with their capacity to regulate oxidative stress and inflammation, both of which play a significant role in the progression of Alzheimer's disease. This is especially pertinent due to the growing acknowledgment of oxidative stress as a contributing element in the onset of Alzheimer's disease.<sup>27</sup> The prospective therapeutic ramifications of *Erythrina* alkaloids in Alzheimer's disease are notably encouraging, with evidence substantiating their neuroprotective attributes and capacity to mitigate oxidative stress. Future research must focus on elucidating the underlying mechanisms of action, executing clinical studies, and investigating the incorporation of this chemical into holistic therapy regimens for Alzheimer's disease.

## Materials and Methods

### Alkaloid Structure Preparation

A comprehensive literature analysis has led to the isolation and identification of a total of 143 alkaloid structures from the genus *Erythrina*.<sup>21</sup> Chemaxon MarvinSketch was used to construct and forecast the two-dimensional (2D) structures and protonated state structures of alkaloids at a physiological pH of 7.4. The protonated state of the three-dimensional

structures was optimized using the Merck molecular force field (MMFF94). The 3D structure in its protonated state at a pH level that is typical for the human body was stored in the.pdb file format.<sup>28</sup> Subsequently, the file was processed by including H atoms, applying Gasteiger charges, and designating rotatable bonds for investigation in the docking procedure. The 3D structure underwent additional processing via molecular docking using AutoDock 1.5.7 tools and was saved in pdbqt format.

## Preparation of Co-Crystallized Proteins and Ligands

Recombinant human acetylcholinesterase in combination with (-)-galantamine crystal structure was acquired from the Protein Data Bank (PDB) (<https://www.rscb.org> accessed on June 25, 2024) with the PDB ID 4EY6.<sup>29</sup> The 3D structure of recombinant human acetylcholinesterase complexed with (-)-galantamine was separated using BIOVIA Discovery Studio (DS) 2020 Client and saved as a separate.pdb file, while water molecules and ions were removed. Next, both structures are inputted into AutoDockTools 1.5.7 for molecular docking validation. Nonpolar hydrogen atoms are discarded, while polar hydrogen atoms are retained. The Gasteiger and Kollman12 atomic charges were added to the structures of galantamine and recombinant human acetylcholinesterase, respectively. The active torsions of the (-)-galantamine structure were determined according to the recommendations provided by AutoDockTools 1.5.7. The structure of recombinant human acetylcholinesterase with (-)-galantamine is stored in.pdbqt format.

## Molecular Docking Validation and Virtual Screening

The generated protein and co-crystallized ligand structures underwent a redocking process with AutoDock Vina (version 1.2.0). The grid box parameter was configured to dimensions of  $36 \times 36 \times 40$  with a spacing of 0.375 Å, including the co-crystallized ligand and the biggest flavonoid structure for docking purposes. The docking postures produced by AutoDock Vina were separated using Vina Split, and the most favorable pose (exhibiting the lowest binding score) was superimposed onto the co-crystallized ligand file. The procedure for validating molecular docking is performed in accordance with the crystal structure of recombinant human, acetylcholinesterase. A total of 143 three-dimensional structures of alkaloids from the genus *Erythrina* were used as targets for docking analysis. Before doing molecular docking for the test compound, it is crucial to first validate the methodology or perform re-docking. At this step, the prepared protein and ligand co-crystals are inserted into the AutoDockTools-1.5.7 application. The generated protein and crystallized ligand structure underwent the redocking procedure using Autodock Vina 1.2.0. The dimensions of the grid for brain docking are set to encompass the entire galantamine structure, with the grid box parameters set at a size of  $36 \times 36 \times 40$  and a spacing of 0.375 Å. This This grid comprises the ligand for crystallization and the primary alkaloid structure for docking. The lattice box is formed by using coordinates parallel to the co-crystal ligand centered on the crystal. The arrangement of this box is such that it allows it to accommodate the largest co-crystal ligands and test ligands.

After the completion of the molecular docking process, an output file of the docking, in.pdbqt format, will be generated. This file contains various poses of test compounds obtained by molecular docking. The next step is to divide the different poses of each compound's docking results into separate files. Upon separating all docking poses, the pose exhibiting the lowest binding energy is accessed in the Biovia Discovery software and superimposed onto the co-crystal ligand file before conducting molecular docking. The docking poses generated by Autodock Vina are separated using Vina Split. This can be achieved by executing the vina split program from the command prompt using the command `vina_split.exe -input`. The optimal docking pose with the lowest binding affinity is superimposed with the ligand file that has been crystallized prior to performing molecular docking to calculate the Root Mean Square Deviation (RMSD) value using Biovia Discovery Studio (DS) 20 Client which resulted in RMSD of 0.3403 Å. The parameter docking of the redocking procedure is employed for the virtual screening of 143 flavonoids against human acetylcholinesterase protein.

## ADMET Prediction and Lipinski's Rule of Five

The pharmacokinetic parameters, including absorption, distribution, metabolism, excretion, and toxicity (ADMET), and Lipinski's Rule of Five (Ro5) calculations are predicted using the online server ADMETlab, which may be accessed at <https://admetmesh.scbdd.com/>. The parameters for assessing drug absorption encompass various factors, including

solubility in water, Caco2 permeability, human intestinal absorption, susceptibility to P-glycoprotein substrates, and the potential for substrates to inhibit P-glycoprotein I and II. When predicting distribution parameters, several factors are taken into account, including steady-state volume of distribution (VDss), unbound fraction, blood-brain barrier (BBB) permeability, and central nervous system (CNS) involvement. Metabolic studies conducted in silico involve predicting the impact of inhibition on CYP1A2, CYP2C19, CYP2C9, and CYP2D6 enzymes. In addition, pkCSM is used to estimate the likelihood of hits that serve as substrates for CYP2D6 and CYP3A4. Excretion mechanism assessment relies on two criteria: overall clearance and interaction with the renal organic cation transporter 2 (OCT2). The security profile evaluation involves the use of ADMETLab 2.0 to predict the toxicity and hepatotoxicity of AMES. In addition, a web server is utilized to assess the potential impact as an inhibitor of the hERG (ether-a-go-go related gene) channels I and II.<sup>30</sup>

The best compound hits obtained from the virtual screening were evaluated for compliance with Rule of Five (Ro5) Lipinski<sup>31,32</sup> using the SwissADME web server (<http://www.swissadme.ch/>). The purpose of this stage is to evaluate the possibility of the hits as medication candidates that can be administered orally and remain effective. Lipinski's Rule of Five (Ro5) assesses potential drug candidates by considering their molecular weight (MW), log P value, as well as the number of hydrogen bond donors (HBD) and acceptors (HBA).

## Molecular Dynamic Simulation

Molecular dynamics simulation for the optimal molecule was performed using Amber20 with GPU acceleration.<sup>33,34</sup> The amino acid residues of AChE were parameterized utilizing the ff19SB force field. The partial atomic charges of the ligands were calculated using the Austin Model 1–Bond Charge Corrections (AM1–BCC) approach within the antechamber module of Amber–Tools21. Supplementary parameters for the ligand were obtained from the Generalized Amber Force Field 2 (GAFF2). The alkaloids derived from the genus *Erythrina*, which have the potential to inhibit acetylcholinesterase, were subjected to additional analysis using molecular dynamics (MD) simulations based on the results obtained from virtual screening and toxicity studies. Molecular dynamics simulations were conducted on the most promising compounds using Amber20 with GPU acceleration, as outlined in our prior research. The AChE amino acid residues were parameterized using the ff19SB force field.<sup>31</sup> The Austin Model 1-Bond Charge Correction (AM1-BCC) approach in the Amber-Tools21 antechamber module determined the ligands' partial atomic charges. The ligand's additional properties, including bond length, bond angle, and dihedral angle, were obtained using the Generalized Amber Force Fields 2 (GAFF2). The leap module in Amber-Tools21 was utilized to resolve the AChE ligand complex with a dimension of 10 Å and to attain a salt concentration of 0.15 M by introducing minute quantities of Na<sup>+</sup> and Cl<sup>-</sup> ions into the system.

The molecular dynamics simulation process begins with two sequential energy minimization steps. For the protein-ligand complex, a restraint of 25 kcal/mol was applied in the first step, followed by 5 kcal/mol in the second minimization step. Following the minimization step, we raised the system temperature to 300 K under 50-ps NVT (Number-Volume-Temperature) conditions before switching to NPT (Number-Pressure-Temperature) conditions. After that, the system density was adjusted to 1 g/cm<sup>3</sup> during the 50-ps period. In subsequent NVT simulations, the restraint on the solute was gradually reduced by 1 kcal mol Å<sup>-1</sup> every 50 ps until it completely disappeared.

## Results

### Virtual Screening and Molecular Docking

A total of 143 alkaloid structures isolated from the genus *Erythrina* were screened against the crystal structure of recombinant human acetylcholinesterase (PDB-ID 4EY6). The binding energies of these alkaloids were compared with those of the recombinant human acetylcholinesterase co-crystal ligand, (-)-galantamine, which is a known inhibitor of human acetylcholinesterase, and with those of acetylcholine, the natural substrate of acetylcholinesterase. From the virtual screening, 55 alkaloids exhibited lower binding energies than that of (-)-galantamine and/or acetylcholine (Table 1). In molecular docking, lower binding energy indicates a more stable and favorable interaction between the compound and the target. Therefore these 55 alkaloids may have potentials to inhibit AChE.<sup>35</sup>



**Table 1** Virtual Screening Data of 55 Alkaloid Compounds From the Genus *Erythrina* That Have Low Binding Energy to Acetylcholinesterase

Name of Compounds	Subclass Alkaloids	Binding Affinity (kcal/mol)
Erythrivarine D (136)	Dimerik	-11.92
Erytharborine B (67)	Dienoid	-11.27
Erythrivarine C (135)	Dimerik	-11.10
Erytharborine A (66)	Dienoid	-10.67
Erythrivarine B (134)	Dienoid	-10.61
10,11-Dioxoerysotramidine (46)	Dienoid	-10.29
Erythrivarine A (133)	Dimerik	-10.23
10 $\beta$ -hidroksi-11 $\beta$ -metoksierysotramidin (54)	Dienoid	-10.12
10,11-dioxoerythraline (41)	Dienoid	-10.06
Erytharbine (50)	Dienoid	-9.986
10,11-Dioxoerythratine (102)	Alkenoid	-9.915
11-Oxoerysopine (29)	Dienoid	-9.751
Erisodin-N-oksida (56)	Dienoid	-9.704
10,11-Dioxoerythratidineone (105)	Alkenoid	-9.66
11-Hydroxyerysotine (84)	Alkenoid	-9.608
Erisotramidin (31)	Dienoid	-9.563
8-Oxo- $\beta$ -Eritroidine (125)	Lactonic	-9.468
8-oxoerymelanthine (128)	16-Azaerythrinan	-9.468
10-Oxoerythrinine (40)	Dienoid	-9.454
Crystamidine (49)	Dienoid	-9.447
11- $\beta$ -Hydroxyerysotramidine (33)	Dienoid	-9.434
Erisodinoformin hidroksida (130)	Dimerik	-9.423
$\alpha$ -Eritroidin (121)	Laktonik	-9.388
Erysotnone (97)	Alkenoid	-9.388
Erisoformin klorida (129)	Dimerik	-9.380
8-Oxoerythrinine (38)	Dienoid	-9.347
Erytharborine H (44)	Dienoid	-9.346
8-Oxoerythraline (37)	Dienoid	-9.238
Erysoflorinone (98)	Alkenoid	-9.220
$\beta$ -Eritroidin (124)	Laktonik	-9.106
Erysodienone (116)	Alkenoid	-9.081
11- $\beta$ -metoksieritralin (25)	Dienoid	-8.985
Erytharborine F (104)	Alkenoid	-8.960
11-Methoxyerythratine (92)	Alkenoid	-8.834
11-Oxoerysotine (28)	Dienoid	-8.795
Erytharborine E (113)	Alkenoid	-8.718
Erisopinoformin hidroksida (131)	Dimerik	-8.708
Cristanines B (93)	Alkenoid	-8.668
11- $\beta$ -Methoxyglucoerysodine (73)	Dienoid	-8.525
Erythratidinone (95)	Alkenoid	-8.507
Epierythratine (89)	Alkenoid	-8.485
11- $\alpha$ -Hidroksierysodin (13)	Dienoid	-8.297
11- $\alpha$ -Hydroxyerythravine (21)	Dienoid	-8.290
11-Hydroxyepierythratine (91)	Alkenoid	-8.129
Metil ester hipaforin (141)	Indole	-8.111
Eritratidin N-oksida (111)	Alkenoid	-8.014
Erythritol (115)	Alkenoid	-7.987
11- $\beta$ -Methoxyerysodine (18)	Dienoid	-7.957
Cristanine F (118)	Alkenoid	-7.809
11- $\beta$ -Hydroxyerysotine (17)	Dienoid	-7.791

(Continued)

**Table 1** (Continued).

Name of Compounds	Subclass Alkaloids	Binding Affinity (kcal/mol)
Erysotrine ( <b>7</b> )	Dienoid	-7.653
Cristanine G ( <b>106</b> )	Alkenoid	-7.593
11- $\alpha$ -Hydroxyerysotrine ( <b>12</b> )	Dienoid	-7.591
1H-Indole-3-propanamide ( <b>144</b> )	Indole	-7.571
Erytharborine D ( <b>108</b> )	Alkenoid	-7.557
(-) -galantamine	Co-crystallized ligand	-10.440
Acetylcholine	Natural ligand	-4.495

## Toxicity Prediction

Toxicology prediction is a fundamental component of the process of determining the potential adverse effects that a given substance may have on human health. It has been demonstrated that continuous exposure to chemicals typically results in genotoxicity, carcinogenicity, immunotoxicity, and reproductive and developmental toxicity in humans.<sup>36,37</sup> The toxic endpoints subjected to evaluation were mutagenicity, hERG inhibition, and hepatotoxicity. Among the 55 alkaloids under consideration, three were identified as being potentially safe with respect to mutagenicity, hERG inhibition, and hepatotoxicity. Based on the 55 structures obtained, these potential AChE inhibitors were evaluated for toxicity. The results indicated that the three alkaloids from the genus *Erythrina* exhibited a low to moderate toxic risk (Table 2). The three compounds were 8-oxoerymelanthine (**128**) and erysophorine chloride (**129**) and 1H-indole-3-propanamide (**144**) (Figure 1).

**Table 2** Toxicity Prediction of 55 Alkaloid Compounds From the Genus *Erythrina* That Have Low Binding Energy to Acetylcholinesterase

Compounds	Toxicity Parameters					
	hERG blocker	H-HT	DILI	Mutagenic	Carcinogenicity	Respiratory Toxicity
<b>136</b>	MR	HR	LR	HR	HR	MR
<b>67</b>	LR	HR	LR	MR	MR	HR
<b>135</b>	LR	HR	LR	LR	HR	MR
<b>66</b>	LR	HR	LR	LR	LR	HR
<b>134</b>	LR	HR	LR	LR	HR	LR
<b>46</b>	LR	HR	HR	HR	HR	HR
<b>133</b>	LR	HR	LR	LR	HR	MR
<b>54</b>	LR	HR	HR	HR	HR	HR
<b>41</b>	LR	HR	MR	HR	HR	MR
<b>50</b>	LR	HR	HR	HR	HR	HR
<b>102</b>	LR	MR	MR	MR	HR	HR
<b>29</b>	LR	MR	MR	HR	HR	HR
<b>56</b>	LR	HR	LR	HR	HR	HR
<b>105</b>	LR	LR	MR	MR	HR	LR
<b>84</b>	LR	MR	LR	MR	MR	HR
<b>31</b>	LR	HR	LR	HR	HR	SDM
<b>125</b>	LR	MR	HR	MR	MR	HR
<b>128</b>	<b>LR</b>	<b>LR</b>	<b>LR</b>	<b>LR</b>	<b>LR</b>	<b>LR</b>
<b>40</b>	LR	HR	MR	HR	HR	HR
<b>49</b>	LR	HR	HR	MR	HR	HR

(Continued)

Table 2 (Continued).

Compounds	Toxicity Parameters					
	hERG blocker	H-HT	DILI	Mutagenic	Carcinogenicity	Respiratory Toxicity
33	MR	HR	HR	HR	HR	HR
130	LR	MR	LR	LR	LR	HR
121	MR	MR	LR	LR	LR	HR
97	LR	MR	LR	HR	HR	LR
129	<b>LR</b>	<b>LR</b>	<b>LR</b>	<b>LR</b>	<b>LR</b>	<b>LR</b>
38	MR	HR	HR	HR	HR	HR
44	LR	HR	LR	MR	HR	HR
37	MR	HR	MR	HR	HR	MR
98	LR	MR	LR	HR	HR	MR
124	MR	MR	LR	LR	LR	HR
116	LR	MR	HR	HR	HR	HR
25	MR	HR	LR	MR	HR	HR
104	LR	MR	LR	HR	HR	MR
92	LR	HR	LR	MR	MR	HR
28	LR	MR	MR	MR	HR	HR
113	LR	LR	LR	MR	HR	HR
131	LR	MR	MR	LR	LR	HR
93	LR	MR	LR	LR	LR	HR
73	LR	HR	LR	LR	LR	HR
95	LR	MR	LR	HR	HR	MR
89	LR	HR	LR	HR	MR	SDM
13	LR	HR	LR	MR	HR	SDM
21	LR	HR	LR	LR	HR	SDM
91	LR	HR	LR	HR	HR	HR
141	MR	HR	HR	HR	MR	MR
111	LR	MR	LR	HR	LR	HR
115	LR	HR	LR	HR	HR	HR
18	MR	HR	LR	HR	HR	HR
118	LR	HR	LR	LR	HR	HR
17	MR	HR	LR	LR	HR	HR
7	LR	HR	LR	MR	HR	HR
106	LR	HR	LR	MR	MR	HR
12	LR	HR	LR	MR	HR	HR
144	<b>LR</b>	<b>MR</b>	<b>LR</b>	<b>LR</b>	<b>LR</b>	<b>MR</b>
108	LR	HR	LR	LR	HR	HR

**Abbreviations:** HR, high risk; MR, moderate risk; LR, low risk, H-HT, human hepatotoxic; DILI, drug-induced liver injury.

## Molecular Dynamics Simulation

From molecular docking and in silico toxicity screening, we identified 8-oxoerymelanthine (128) as a potential AChE inhibitor with a low toxicity profile. To further evaluate the potency of 128 as an AChE inhibitor candidate, this compound was subjected to molecular dynamics simulation. The result can be described in terms of Root Mean Square Deviation (RMSD), Root Mean Square Fluctuation (RMSF), and MMGBSA Free Energy Calculation.

### Root Mean Square Deviation (RMSD)

The RMSD values of the Apo form along with AChE-ACh complex, AChE-GNT complex, and AChE-**128** complex are given in Figure 2. The apo state of acetylcholinesterase (AChE) shows the highest RMSD, with a mean value of 1.673 Å and a mean absolute deviation (MAD) of 0.321 Å. While the AChE-**128** complex showed a low RMSD almost close to



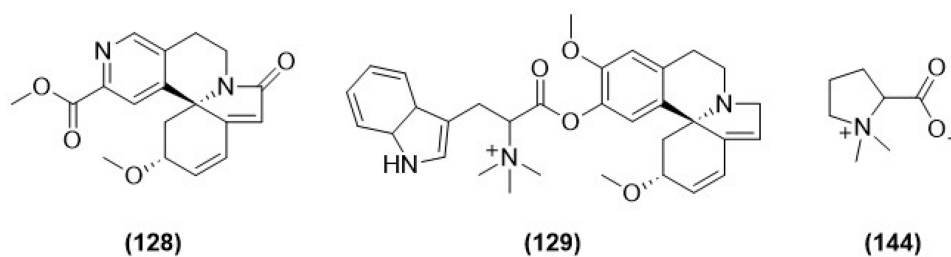


**Figure 1** Structures of compounds (128), (129), and (144).

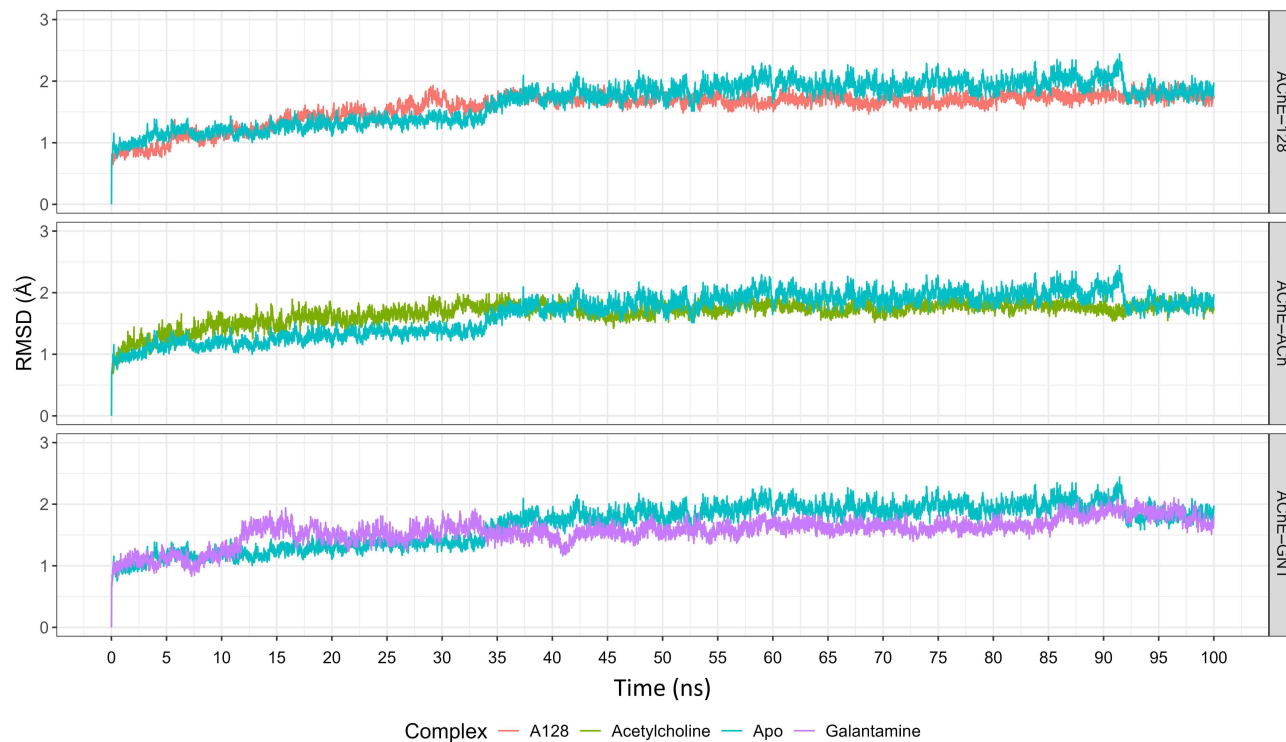


**Figure 2** RMSD plot of AChE–compound **128** complex (cyan-red), AChE–galantamine complex (purple), AChE–acetylcholine (green), and AChE apo form (blue).

galantamine (mean value = 1.584 Å and MAD = 0.138 Å), when compared to the AChE-Apo and AChE-ACh complexes (as shown in Table 3). Compound **128** shows good stability with relatively low RMSD values, more stable than Apo and Acetylcholine, but has almost the same RMSD value but lower than Galantamine.

**Table 3** RMSD Data of Compound **128**, Apo State, Acetylcholine, and Galantamine

Variables	Median	MAD	Mean
Apo	1.783	0.321	1.673
Acetylcholine	1.721	0.127	1.674
Galantamine	1.592	0.150	1.562
Compound <b>128</b>	1.671	0.138	1.584

### Root Mean Square Fluctuation (RMSF)

The RMSF values of the AChE-**128** complex, along with AChE-GNT, AChE-acetylcholine, and the Apo form of AChE, are given in Figure 3. The overall RMSF value of compound **128** is smaller than that of Acetylcholine and Galantamine, indicating that **128** has more stable residue regions. When compared to the state of Apo, the RMSF value of compound **128**, although it has some significant fluctuation peaks, is overall lower than Apo. Upon closer inspection of the 100 ns trajectories within various structural regions, including the triad, omega loop, and George entry, significant differences emerged between the apo (unbound) form and the ligand-bound form of AChE. Compound **128** has the ability to stabilize residues near the binding site better than Acetylcholine and Apo.

### MMGBSA Free Energy Calculation

The Molecular Mechanics Generalized Born Surface Area (MMGBSA) analytical approach quantifies the Gibbs free energy ( $\Delta G$ ) value obtained from ligand-receptor complex stability evaluation. A highly negative  $\Delta G$  value signifies a more robust and enduring interaction between the ligand and receptor. The stability of ligand-receptor complexes was assessed in this work by the use of the Molecular Mechanics Generalized Born Surface Area (MMGBSA) theory in molecular dynamics simulation.<sup>38</sup> MMGBSA  $\Delta G$  calculations from molecular dynamics simulation trajectories explained that compound **128**, compared to galantamine (a well-known AChE inhibitor) and acetylcholinesterase (an AChE native substrate), had the lowest binding energy (Figure 4), with the lowest Gibbs free energy, indicating that this ligand-receptor complex is more stable compared to other ligands.

To evaluate whether there were significant differences among the three complexes, we performed the Kruskal–Wallis rank sum test, followed by Dunn’s multiple comparison test using the Bonferroni method as a post hoc test.<sup>34</sup> This study showed that compound **128** had the highest stability in binding to the receptor based on the  $\Delta G$  value of the MMGBSA analysis, followed by galantamine and acetylcholine (Figure 4).

### Pharmacokinetics and Lipinski’s Rule of Five

After toxicity screening and molecular dynamics simulation of the alkaloid compounds, we performed pharmacokinetic evaluation of the best-hit non-toxic alkaloid compounds through in silico studies summarized in Table 4. The **128** best-hit

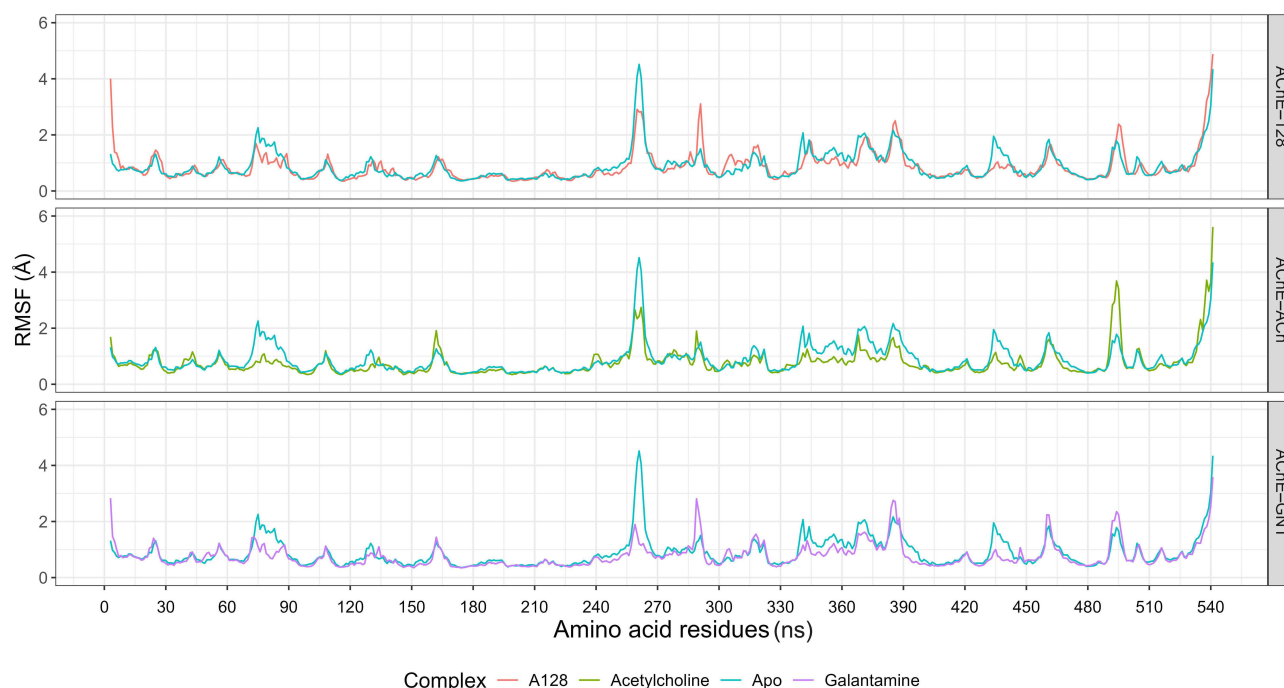


**Figure 3** RMSF plot of AChE-compound **128** complex (cyan-red), AChE-galantamine complex (purple), AChE-acetylcholine (green), and AChE apo form (blue).

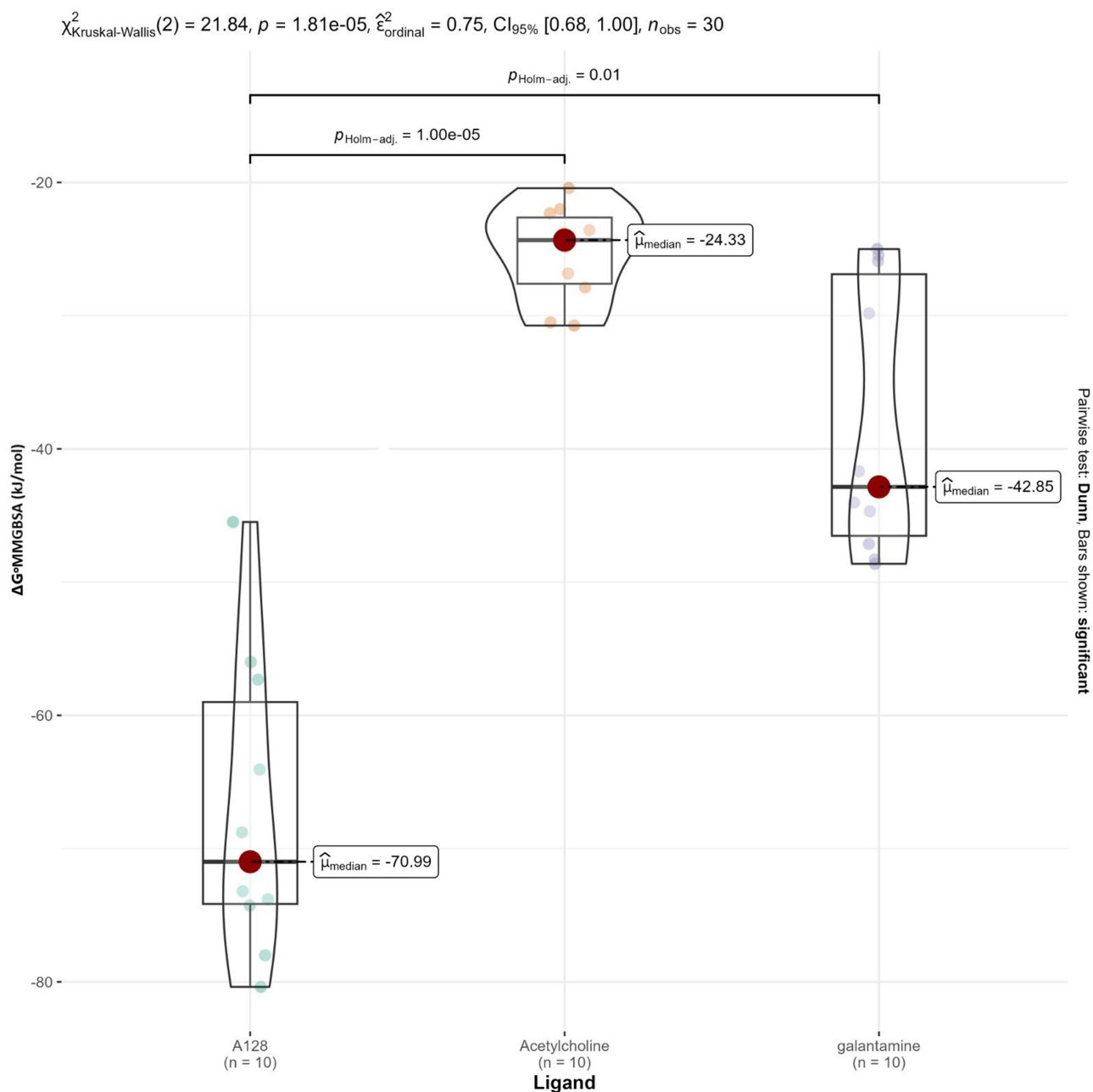


**Figure 4** Box and violin plots illustrating  $\Delta G^{\circ}$  MMGBSA values for ligand binding to AChE. Data points were derived from ten  $\Delta G^{\circ}$  MMGBSA calculations within a 10-ns sliding window across 100-ns trajectories. Statistical significance was assessed using the Kruskal–Wallis rank sum test followed by Dunn’s multiple comparisons test.

alkaloid compounds were further assessed for drug similarity using Lipinski’s Rule of Five (Ro5) through the SwissADME web server. The **128** best-hit alkaloid compounds met the Ro5 minimum requirements, with MW 246.30 g/mol, number of HBD of 1, number of HBA of 2, log P value less than 5, and molar refractivity value of 69.50. These results indicate that the alkaloid compound **128** is a drug-like molecule and an orally active drug candidate.

## Statistical Analysis

Statistical analysis was performed using R programming language.<sup>39</sup>

**Table 4** Pharmacokinetic Prediction of Compound 128

Pharmacokinetic Parameters	Compound 128
<b>Absorption</b>	
Permeabilitas Caco-2 Permeability	-5.505
Permeabilitas MDCK Permeability	1.4e-05
Pgp inhibitors	Low probability
Pgp-substrate	Low probability
Human intestinal absorption	High
<b>Distribution</b>	
Plasma protein binding (PBP)	11.997%
Volume distribution (VD)	0.817
BBB Penetration	Medium penetration
Unbound fractions	84.737%
<b>Metabolism</b>	
CYP1A2 inhibitors	No.
CYP1A2 substrate	Yes.
CYP2C19 inhibitors	No.
CYP2C19 Substrate	No.
CYP2C9 inhibitors	No.
CYP2C9 Substrate	Yes.
CYP2D6 inhibitors	No.
CYP2D6 substrate	Yes.
CYP3A4 inhibitors	No.
CYP2A4 substrate	No.
<b>Excretion</b>	
Total clearance	3.090

## Discussion

Alzheimer's disease is a chronic neurodegenerative disease that is becoming one of the biggest global health problems, with a significant increase in cases every year. Currently available therapies and treatments have many side effects with effectiveness that decreases over time, so new therapeutic agents that are more effective and safer are needed.<sup>38</sup> Alkaloids are a group of natural substances found as important components of plants that exhibit significant biological, pharmacological, and physiological effects. Alkaloid compounds from the genus *Erythrina* have significant potential as AChE inhibitors, which can be further developed as a therapy for AD.<sup>40</sup> A total of 143 alkaloid structures that have been isolated from the genus *Erythrina* were screened against the crystal structure of recombinant human acetylcholinesterase (PDB-ID 4EY6). The binding affinities of these alkaloids were compared to the recombinant human acetylcholinesterase co-crystal ligand, (-)-galantamine, which is a known inhibitor of human acetylcholinesterase. The binding affinity of this alkaloid was compared with that of the recombinant human acetylcholinesterase co-crystal ligand, ie, (-)-galantamine, which is a known inhibitor of human acetylcholinesterase. Their binding affinity was also compared with acetylcholine, the natural substrate of acetylcholinesterase. Among the 143 alkaloid compounds that have been subjected to virtual screening through molecular docking, the top 55 compounds that have lower binding affinity than (-)-galantamine and/or acetylcholine (Table 1).

These compounds have lower binding affinity compared to (-)-galantamine, which is an acetylcholinesterase inhibitor. Some of these alkaloids have excellent binding energy values. Compounds that have lower binding affinity show greater potential for inhibiting AChE, as they are able to interact more strongly with the active site of the enzyme. Low binding affinity is a key indicator of the potency of an effective AChE inhibitor. This is important within the framework of Alzheimer's disease, the inhibition of AChE may potentially enhance the levels of acetylcholine in the brain, thereby

leading to beneficial effects on cognitive performance in affected individuals.<sup>41</sup> The identification of the top 55 alkaloid compounds based on their lower binding affinity compared to (-)-galantamine and/or acetylcholine is an important part of the process of assessing potential compounds for further research in the context of drug development or biochemical research. The compounds fall into the subclasses of dimeric alkaloids, dienoids, alkenoids, lactonics, indoles, and 16-azaeritran. The virtual screening campaign conducted showed that many alkaloids from the genus *Erythrina* have potential as acetylcholinesterase inhibitors. Nevertheless, these molecules must meet the drug similarity criteria in order to be effective as oral medications. Thus, in the subsequent stage, the best-hit compounds obtained were evaluated for toxicity using the SwissADME online server.

Toxicology prediction is essential to establish the potential negative effects that a substance may have. This is because continuous exposure to chemicals usually results in genotoxicity, carcinogenicity, immunotoxicity, and reproductive and developmental toxicity in humans. To evaluate the risks posed by chemicals or drug candidates, toxicity assessment requires in vitro, in vivo, and in silico techniques.<sup>36,37</sup> The assessed toxicological endpoints include mutagenicity, suppression of hERG, and hepatotoxicity. Mutagenic medications refer to pharmaceutical compounds that have the potential to cause genetic alterations or genotoxic consequences in personnel who are exposed to them.<sup>42</sup> Screening for hERG inhibitors is a crucial stage in pharmaceutical research aimed at identifying substances capable of inducing cardiac arrhythmias via the inhibition of hERG channels. The hepatotoxicity of hERG inhibitors is a significant factor contributing to the withdrawal of drugs from the pharmaceutical market and hindering the progress of novel molecule development.<sup>43</sup> Toxicity prediction is a critical step in drug development, especially to ensure that the identified potential compounds do not cause harmful side effects in patients. The 55 alkaloid compounds from the genus *Erythrina* selected based on their binding affinity to AChE were further evaluated for their toxicity profile using an in silico approach. A total of 55 alkaloid compounds were subjected to in silico toxicity screening to estimate their toxicity capabilities, encompassing hERG inhibitors, human hepatotoxicity, drug-induced liver damage (DILI), mutagenicity, carcinogenicity, and respiratory toxicity. Among the 55 alkaloid compounds, no compounds were predicted to have a high risk as hERG inhibitors. Among the compounds assessed, 34 were identified as having a significant risk of hepatotoxicity, 9 as having a high risk of causing drug-induced liver injury (DILI), 23 as having a high risk of mutagenicity, 37 as having a high risk of carcinogenicity, and 40 as having a high risk of respiratory toxicity. Based on the 55 structures obtained, these potential AChE inhibitors were evaluated for toxicity, and we found that three alkaloid compounds from the genus *Erythrina* showed low to moderate toxic risk (Table 2).

Among the 55 alkaloids evaluated, three compounds showed the lowest toxicity profile and were predicted to be safe for further development. A total of three were predicted to be safe from mutations, hERG inhibitors, and hepatotoxicity. The compounds were 8-oxoerymelanthine (**128**) and erysophorine chloride (**129**) and 1H-indole-3-propanamide (**144**) (Figure 1). Among the three alkaloids obtained, the best hit with lower binding affinity than galantamine (GNT) and predicted to show low toxicity was identified. The top-hit alkaloid compound 8-oxoerymelanthine (**128**) was further analyzed by molecular dynamics to evaluate the stability of AChE after binding with these compounds, followed by in silico pharmacokinetics and drug similarity prediction to evaluate the potential of these compounds to be developed as potential drugs for AD therapy.

Based on the three best compounds obtained, the best hits were evaluated for further analysis with molecular dynamics. The results can be described in terms of free binding energies (RMSD, RMSF, and MMGBSA). Lower RMSD values indicate that the system structure remains closer to the reference structure, which signifies better stability. RMSD analysis measures the average deviation from the initial structure throughout the simulation time. The RMSD gives an idea of the global change in conformation.<sup>44,45</sup> RMSD is used to measure the global structural similarity of macromolecules after roto-translational least-squares fitting.<sup>46</sup> The RMSD values of the Apo form along with the AChE-ACh complex, AChE-GNT complex, and AChE-**128** complex are given in Figure 2. The apo state of acetylcholinesterase (AChE) showed the highest RMSD, with a mean value of 1.673 Å and a mean absolute deviation (MAD) of 0.321 Å. While the AChE-**128** complex showed a low RMSD almost close to galantamine (mean value = 1.584 Å and MAD = 0.138 Å), when compared to the AChE-Apo and AChE-ACh complexes (Table 3).

Compound **128** shows good stability with a relatively low RMSD value, more stable than apo and acetylcholine, but has an RMSD value that is almost the same and lower than galantamine. The RMSD plot (Figure 2) shows that

compound **128** stabilizes the AChE protein due to the AChE-**128** complex, shown with an average value of 1.584 Å and MAD of 0.138 Å (Table 3). Compound **128** has almost the same RMSD value as galantamine, indicating that complex has high stability with a low RMSD value but is not as good as galantamine. The interaction between compound **128** and the protein is strong enough to maintain stability, but there may be some factors that cause small shifts in the structure. Ligands that can form strong, stable interactions with the protein (such as galantamine and compound **128**) are better able to keep the protein conformation close to the initial reference structure, reduce fluctuations, and provide higher stability throughout the simulation. In the analysis, it should be noted that lower RMSD values indicate greater stability in the biomolecular structure during these interactions.<sup>47</sup> The stability of the AChE-**128** complex is further supported by the RMSF plot. The lower RMSD value and better stability throughout the simulation indicate that the compound **128**-receptor complex is more stable compared to galantamine and acetylcholinesterase. Therefore, in terms of residue structure stability, compound **128** showed lower fluctuations and was more stable compared to apo, acetylcholine, and galantamine.

RMSF (Root Mean Square Fluctuation) measures the average fluctuation of atomic positions in residues throughout the simulation, providing insight into the local flexibility of residues in a protein. RMSF analysis measures fluctuations by calculating the root mean square deviation of the atomic positions from their equilibrium positions.<sup>48</sup> RMSF plots serve as a general representation for residues that have undergone substantial changes during MD simulations.<sup>49</sup> The RMSF values of the AChE-**128** complex, along with AChE-GNT, AChE-acetylcholine, and the Apo form of AChE, are given in Figure 3. The overall RMSF value of compound **128** is smaller compared to acetylcholine and galantamine, indicating that compound **128** has more stable residue regions. When compared to the state of Apo, the RMSF value of compound **128**, although it has some significant fluctuation peaks, is overall lower than Apo. Upon closer inspection of the 100 ns trajectories within various structural regions, including the triad, omega loop, and George entry, significant differences emerged between the apo (unbound) form and the ligand-bound form of AChE. Compound **128** has the ability to stabilize residues near the binding site better than acetylcholine and apo. This could be due to the stronger interaction and better fit to the protein binding site, thus stabilizing the residues near the binding site.

The RMSF plot for compound **128** shows that most residues have low to moderate fluctuations (0–2 Å), and some residues show higher fluctuations (above 3 Å), which may be in loops or more flexible surface regions. The results of RMSF analysis on acetylcholinesterase (AChE) provide deep insights into the dynamics and stability of key domains in this enzyme, especially in the context of ligand binding of compounds **128**, acetylcholine, and galantamine. The catalytic triad domain, consisting of serine, histidine, and glutamate residues, plays a major role in the hydrolysis process of acetylcholine, such as HIE447. The catalytic domain contains the catalytic site and is located at the base of the active gorge. It is responsible for the formation of acyl-enzyme intermediates that are important in the catalytic mechanism and facilitate the occurrence of acetylcholine hydrolysis. The catalytic site of AChE is located at the base of a deep and narrow active gorge, which enables high catalytic efficiency despite its complex architecture.<sup>50,51</sup> The low RMSF value around the catalytic domain indicates high stability for enzymatic activity. The stability of this domain is important to ensure an efficient catalytic reaction.<sup>52</sup> When AChE interacts with ligand **128**, the stability around this domain generally increases, indicating the conformational locking required for effective enzyme inhibition.

While the oxyanion hole of AChE plays an important role in stabilizing the transition state during the catalytic reaction. The low RMSF of these residues indicates the stability required to hold the transition state and prevent fluctuations that could disrupt catalysis.<sup>53,54</sup> The active site domain is gorged with key residues such as TRP86, TYR337, and GLU202. The low RMSF value indicates that the residues in the active site gorge have little fluctuation and can be interpreted as a sign of high structural stability. Fluctuations in the active site gorge facilitate substrate binding and release. The flexibility required for ligand or substrate binding and release is based on the fluctuations measured along the active gap.<sup>55,56</sup> The Peripheral Anionic Site (PAS) domain is a crucial region in AChE that plays an important role in enzyme function and inhibition. This domain is critical to understanding how stability and flexibility affect the overall function of AChE.<sup>57</sup> Residues in the Peripheral Anionic Site include TRP86 and TYR337. Residues in PAS that exhibit low RMSF tend to be more stable, indicating that PAS can effectively maintain the conformation required for substrate or inhibitor binding.



Key residues from AChE domains such as TRP86, TYR337, TYR133, HIE447, GLU202, and SER203 play a crucial role in the binding of acetylcholine at the active site of Acetylcholinesterase (AChE) (Figure 5). These residues ensure that acetylcholine is firmly bound, in the right conformation, and ready to undergo the catalytic reaction. TRP86 and TYR337 provide hydrophobic stabilization through pi interactions, while residues TYR133 and HIE447 support orientation and catalysis of hydrolysis reactions. Residues GLU202 and SER203 play a role in orienting and breaking down acetylcholine molecules. These overall interactions allow AChE to efficiently perform its function of breaking down acetylcholine, which is key in the regulation of synaptic transmission in the nervous system.

Key residues such as TRP86, TYR337, TYR133, HIE447, GLY120, GLU202, and SER203 play an important role in the pharmacophore interaction of galantamine and candidate inhibitor compound **128** with the acetylcholinesterase enzyme, which will form conventional hydrogen bonds and significant pi-alkyl interactions. These residues help stabilize the position of the compound within the active site, ensuring effective inhibition of the enzyme. This bonding allows galantamine to increase acetylcholine levels in the nerve synapse, which is important for improving cognitive function in Alzheimer's patients. In compound **128**, residues such as TRP86, TYR337, TYR133, HIE447, GLY120, GLU202, and SER203 also play an important role in forming interaction patterns similar to galantamine, including hydrogen and pi-alkyl bonds. Compound **128** shows interactions with residues such as TRP, TYR, HIE, SER, GLY, and GLU with similar interaction patterns but not completely identical to galantamine. In both compounds, pi-alkyl and pi-stacked interactions were seen, suggesting that they interact with target proteins through a mechanism involving aromatic rings. These interactions make an important contribution to the binding affinity and specificity of both compounds with the enzyme.<sup>58</sup> The similarity in the type and location of these interactions suggests that compound **128** has the potential to mimic the binding mechanism of galantamine, which could make it a promising alternative candidate as an acetylcholinesterase inhibitor. The galantamine compound and candidate inhibitor compound **128** form conventional hydrogen bonds that are important for the stabilization of the molecule within the active site. For example, hydrogen interactions involving residues such as SER and TYR on galantamine can also be found on compound **128**, indicating that these two compounds are capable of forming similar bonds with the same part of the enzyme (Figure 5).

A side-to-side comparison of the interactions formed by the galantamine inhibitor with the candidate inhibitor compound **128** revealed that both compounds Both compounds exhibit interactions involving conventional hydrogen, pi-alkyl, and Van der Waals bonds. Although there are some recurring residues in both interactions (such as TYR and PHE),

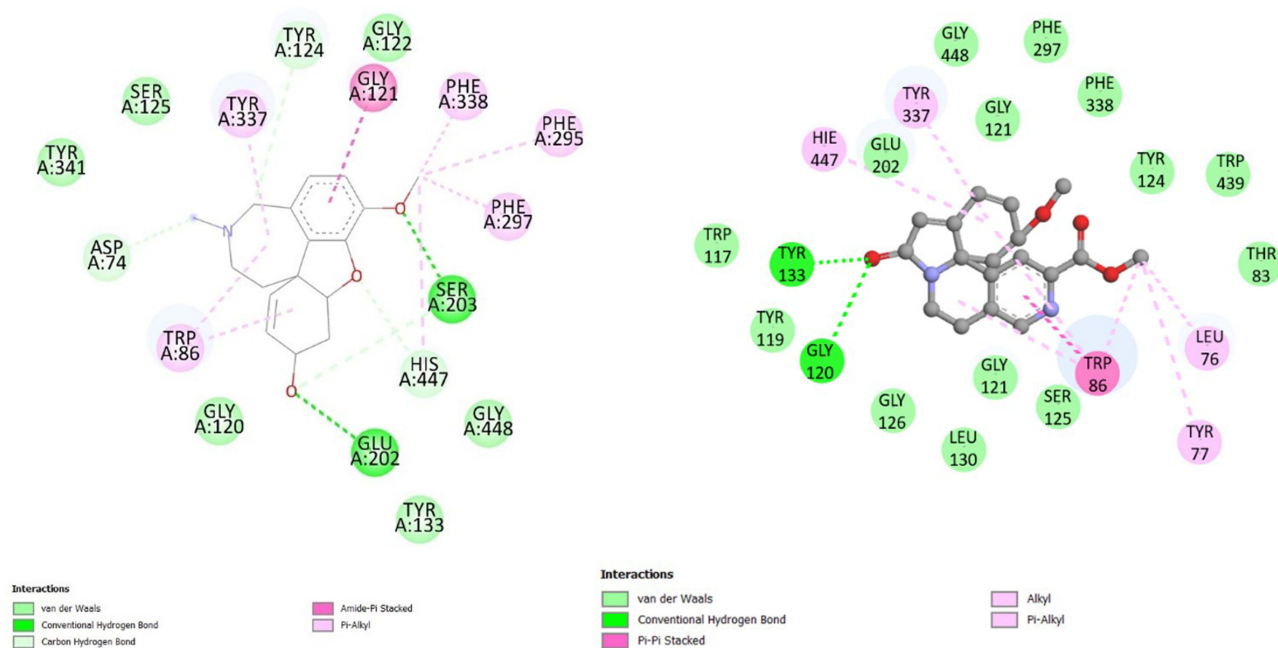


**Figure 5** The 2D representation of galantamine (left) and **128** (right) interaction with active site of AChE.

the specific residues involved are different. This suggests that the two inhibitors have different binding modes, even though they both bind to the same active site. Conventional hydrogen and Pi-Pi-stacked interactions are often stronger and more specific than Van der Waals or Pi-Alkyl interactions. Compound **128** may have stronger binding to AChE than galantamine, specifically through Pi-Pi-stacked interactions. Based on the interactions seen, compound **128** might show higher affinity towards AChE compared to galantamine, as it has more specific types of interactions, such as Pi-Pi Stacked.

Galantamine's pharmacophore focuses on hydrogen interactions and aromatic interactions with one main benzene ring, making it an effective but possibly less flexible inhibitor. However, compound **128** exhibits a more complex pharmacophore with more aromatic rings, increasing Pi-Pi interactions and possibly providing greater structural flexibility. This makes compound **128** potentially more effective as an AChE inhibitor than galantamine, due to its ability to form more and stronger interactions with the enzyme target. Aromatic interactions (Pi-Pi interactions) in galantamine rely on one aromatic ring that interacts with aromatic residues in AChE. Whereas compound **128** has two or more aromatic rings that can potentially increase the number and strength of Pi-Pi interactions, especially stacked Pi-Pi interactions, which are more stable. Galantamine donors and acceptors feature hydrogen donors and acceptors involved in multiple hydrogen bonds, important for bonding affinity. Whereas compound **128** has hydrogen donors and acceptors, their contributions may be more focused on non-covalent interactions such as Pi-Pi. The structure and flexibility of galantamine are relatively rigid, with a cyclohexane ring and a single aromatic ring, which might limit some aspects of interaction with AChE. However, with compound **128** having more aromatic rings and possibly a more flexible structure, these compounds may be better able to conform to the AChE active site and form more interactions.

The inhibitor compound **128** has significant structural similarities with galantamine, especially in terms of orientation and position relative to the target (Figure 6). Galantamine and the inhibitor compound **128** have fairly close positions, which suggests that they may interact with the target residues at the same or similar places, especially at their aromatic nuclei. This signifies that the two compounds are likely to occupy the same space within the active site of the target enzyme. The overlap seen in the major parts of the core structure (especially the aromatic ring) indicates that they may bind at similar binding sites with similar interaction mechanisms. The orientation of the aromatic rings in both compounds looks similar, which is an important indicator that they may interact with the same target active site or at least have similar binding mechanisms.

The Molecular Mechanics Generalized Born Surface Area (MMGBSA) analysis approach quantifies the Gibbs free energy ( $\Delta G$ ) value obtained from ligand-receptor complexes to assess their stability. Stronger and more persistent contact

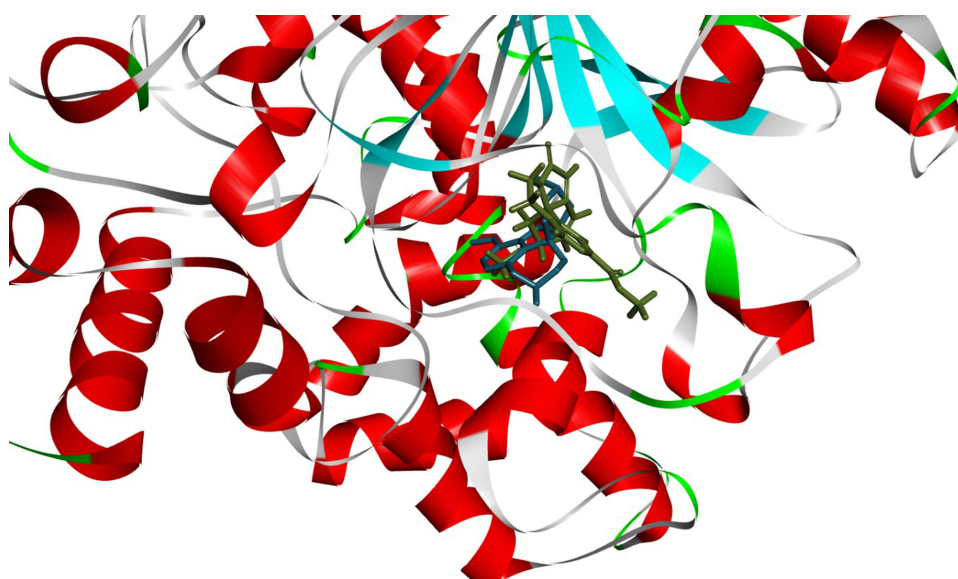


**Figure 6** Structural overlay of galantamine (blue) and compound **128** (green) within the binding site of acetylcholinesterase (AChE).

between the ligand and receptor is indicated by a larger negative  $\Delta G$  value. The stability of ligand-receptor complexes was assessed in this work by applications of the Molecular Mechanics Generalized Born Surface Area (MMGBSA) approach in molecular dynamics simulations.<sup>38</sup> MMGBSA  $\Delta G$  calculations from molecular dynamics simulation trajectories explained that compound **128**, compared to galantamine (a well-known AChE inhibitor) and acetylcholinesterase (AChE native substrate), had the lowest binding energy (Figure 4), with the lowest Gibbs free energy, indicating that this ligand-receptor complex is more stable compared to other ligands.

Therefore, to evaluate whether there is a significant difference among the three complexes, the Kruskal–Wallis rank sum test was performed. This test was followed by Dunn’s multiple comparison test using the Bonferroni method as a post hoc test.<sup>34</sup> The study showed that compound **128** had the highest stability in binding to the receptor based on the  $\Delta G$  values from MMGBSA analysis, followed by galantamine and acetylcholine. This difference was statistically significant, indicating the potential of **128** as a potent and stable ligand for pharmacological applications (Figure 4). Therefore, compound **128** has potential as an AChE inhibitor.

MMGBSA free energy calculations of compound **128** showed that it has a much lower binding energy compared to galantamine and AChE. Compound **128** has the highest stability in binding to the receptor (most negative  $\Delta G$ ), followed by galantamine and then acetylcholine. The MMGBSA analysis gave a median  $\Delta G$  value for compound **128** of  $-70.99$  kJ/mol, acetylcholine of  $-24.33$  kJ/mol, and galantamine of  $-42.85$  kJ/mol. Compound **128** has the most negative  $\Delta G$  value, indicating that this ligand-receptor complex is the most stable compared to other ligands. This high stability may be due to the stronger and more favorable interaction between compound **128** and the active site of the receptor. Compound **128** had the lowest median  $\Delta G$  value ( $-70.99$  kJ/mol), which means that the AChE residues help to stabilize the complex with the ligand by providing more energy. The distribution range of  $\Delta G$  values for compound **128** is quite narrow, indicating that the interaction between compound **128** and AChE residues is quite stable and consistent at various simulation positions. Energy decomposition analysis using the MMGBSA (Molecular Mechanics Generalized Born Surface Area) method of various residues in the AChE protein within a certain time range can identify residues that contribute greatly ( $\Delta G$  MMGBSA value  $< -4$  kcal/mol) as key residues in protein or ligand interactions (Figure 7).

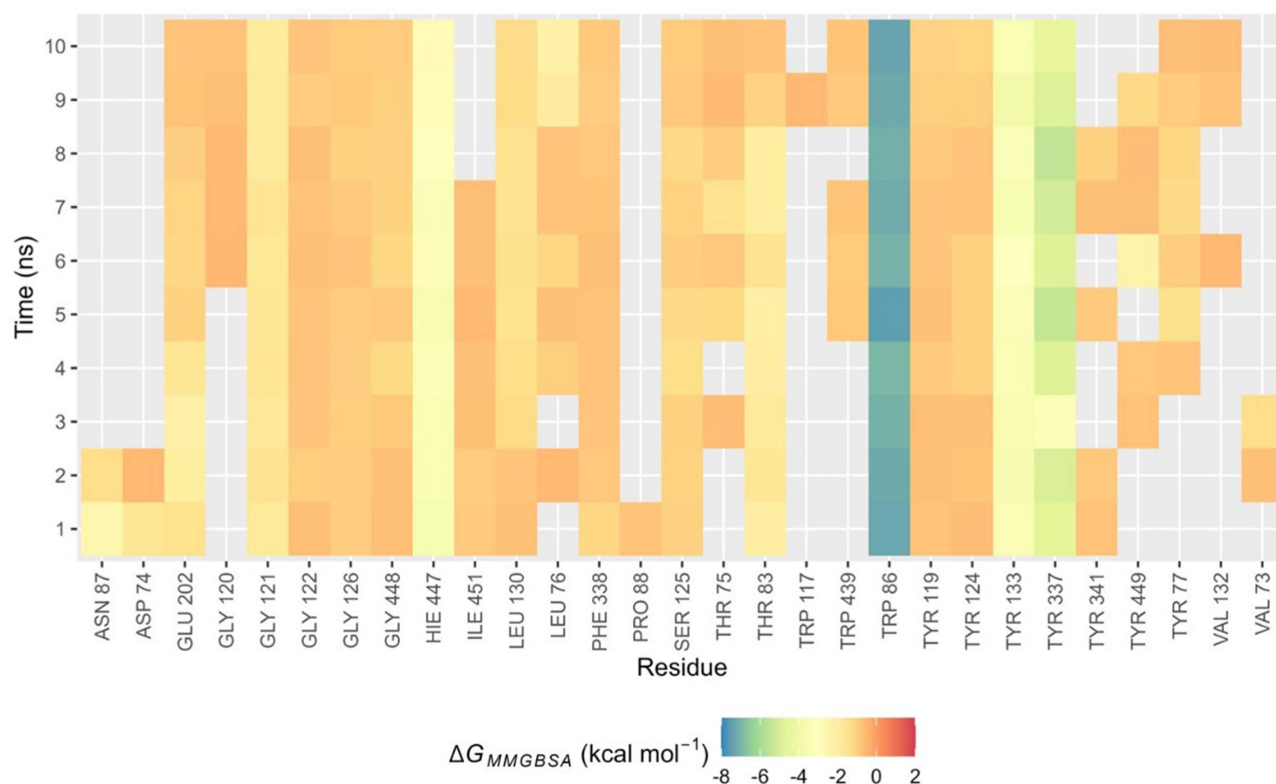


**Figure 7** Heatmap of Residue-Based Free Energy Changes ( $\Delta G$  MMGBSA) Over Time for **128** System.

Energy decomposition analysis of MMGBSA revealed that the key residues in AChE that play vital roles in the stabilization of protein-ligand complexes are TRP86, TYR133, TYR337, and HIE447. The key residue TRP86, which has the highest van der Waals energy contribution (−4402 kcal/mol) and the lowest total energy (−7310 kcal/mol), forms the center where the ligand binds to the AChE active site. Strong hydrophobic forces keep the interaction stable. Residues TYR133 and TYR337 also make important contributions, each with stable electrostatic and van der Waals energy contributions. Residue TYR133 showed significant electrostatic interactions (−4.397 kcal/mol), possibly through the formation of hydrogen bonds that cement the orientation of the ligand in the active site. At the same time, residue HIE447, which has a moderate van der Waals energy contribution (−1.674 kcal/mol), helps keep the active site environment good for ligand binding. Taken together, these residues not only ensure the stability of the complex but also guide the design of more specific and effective AChE inhibitors, with the potential of slowing the progression of AD through stronger and more selective binding to the target enzyme.

The Kruskal–Wallis statistical test showed a significant difference between these three ligands with  $\chi^2 = 21.84$  and a p-value of  $1.81 \times 10^{-5}$ , with a significant difference between the median Gibbs free energy ( $\Delta G$ ) of the three ligands. Further analysis by Dunn's test with Holm's correction showed significant differences between some pairs of ligands, indicated by horizontal lines and adjusted p-values (Holm-adj)<sup>34</sup> (Figure 4). This finding suggests that the binding of **128** is more favorable compared to galantamine and acetylcholinesterase and thus may indicate activity and the potential for inhibition against AChE. Based on the results of molecular dynamics simulations and toxicity studies, it is evident that compound **128** could have potential as an AChE inhibitor and be a potential drug candidate. Therefore, in the next step, we performed in silico pharmacokinetics to predict the pharmacokinetic properties and predicted Lipinski's rule of five calculation. Pharmacokinetics refers to the temporal progression of medication concentration in the body following its delivery. The processes encompassed in this category are absorption, distribution, metabolism, and excretion (ADME). Lipinski's rule of five prediction assesses the resemblance between drugs and identifies if a chemical molecule with a certain pharmacological activity possesses physical and chemical characteristics that qualify it as an orally active drug in humans.

Pharmacokinetic evaluation is a scientific discipline that investigates the movement of foreign chemicals in the body, which includes absorption, distribution, metabolism, and excretion.<sup>59</sup> Evaluation of the pharmacokinetic profile of a drug candidate is an important step in the drug development process, which is crucial at any stage of drug candidate development. This technique can help prevent potential failures in clinical trials by allowing precise prediction of pharmacokinetic characteristics. Anticipating these characteristics in the early stages of pharmaceutical design and development can help prevent setbacks in subsequent clinical trials of potential drugs.<sup>60</sup> Therefore, for potential alkaloid compounds with low to moderate toxicity endpoints, we continue to evaluate their pharmacokinetic parameters in silico. The toxicity evaluation approach can be used to predict pharmacokinetics for decision-making in the development and potential of a new drug candidate compound. The toxicity screening and molecular dynamics simulation of the alkaloid compounds was followed by the pharmacokinetic evaluation of the best hit non-toxic alkaloid compounds (**128**) through in silico studies (Table 4).

Alkaloid compounds **128** with the highest number of hits were evaluated for drug similarity using Lipinski's Rule of Five (Ro5) through the SwissADME web site. As per Ro5, the medicine must possess a molecular weight (MW) below 500 Daltons (Da), a hydrogen bond density (HBD) and a hydrogen bond anion (HBA) below 5 and 10, respectively, and a logP value below 5. The compound must satisfy the three necessary criteria to be classified as a drug-like molecule.<sup>32,40</sup> The best-hit compound **128** alkaloids met the Ro5 minimum requirement, with MW of 246.30 g/mol, number of HBD of 1, number of HBA of 2, log P value less than 5, and molar refractivity value of 69.50. These results indicate that the alkaloid compound **128** is a drug-like molecule and an orally active drug candidate.

The pharmacokinetic and toxicity characteristics of prospective drug candidates should be considered early on to reduce the failure rate during the clinical phase of drug discovery. Undesirable pharmacokinetics and toxicity are crucial elements contributing to the expensive late stages of drug development failure.<sup>61</sup> In terms of drug absorption parameters, the prediction model shows that compound **128** has a Caco-2 and MCDK permeability with a medium value range. This permeability indicates the ability of the compound to pass through Caco-2 cells, which is a model for intestinal absorption. The value indicates low-to-medium permeability but means that the compound is able to penetrate the



intestinal wall. On the other hand, the medium MDCK permeability implies that a compound can cross the renal tubular epithelium, or permeability, through MDCK cells. Compound **128** has values with medium Caco-2 and MDCK permeability, which have the potential to be well absorbed and easily eliminated, making it a potential candidate for drug development.<sup>62</sup> Predictions on Pgp inhibitors and substrates show that compound **128** is predicted to have a low probability as a Pgp inhibitor and as a Pgp substrate. This suggests that compound **128** does not inhibit Pgp and is not pumped out by Pgp. This is advantageous as it reduces the risk of adverse drug interactions and increases the plasma stability and effectiveness of the compound. The compound will not be affected by Pgp activity pumping the drug out of the cell, so it can achieve higher and more stable concentrations in the systemic circulation and target tissues.<sup>63</sup> In addition, compound **128** is predicted to have high human intestinal absorption.

Pharmacokinetics is a crucial factor in characterising the distribution of unmetabolized medications from the circulatory system to different tissues in the body.<sup>64</sup> Pharmaceutical distribution factors assessed in a computer model include plasma protein binding, volume distribution, blood-brain barrier penetration, and the proportion of unbound drugs. Assessment of prospective drug distribution characteristics is crucial, since it significantly influences the degree to which target organs are exposed to the medication.<sup>65</sup> Drug distribution in pharmacokinetics refers to the reversible movement of a drug from one location to another in the body. Upon entering the systemic circulation by absorption or direct administration, a medication must be adequately disseminated into the interstitial and intracellular fluids.<sup>66</sup> The prediction of compound **128** shows that the compound has an appropriate volume of distribution in the range of 0.04–20 L/kg, which is 0.817 L/kg.

The predicted model showed that compound **128** had an appropriate volume of distribution in the range of 0.04–20 L/kg. With a blood-brain barrier (BBB) permeability value that falls under medium penetration. The BBB is a selectively semipermeable membrane in the brain, consisting of tight junctions. The BBB acts as a protective barrier, limiting the passage of certain substances from the bloodstream to the central nervous system (CNS).<sup>67</sup> This ability is very important in treating CNS disorders such as Alzheimer's. The predicted results suggest that compound **128** with meaningful medium penetration can cross the BBB and have potential for neurological applications. The unbound fraction represents the proportion of free drug in plasma, which refers to the percentage of drug that is not bound to plasma proteins and is available to interact with biological targets. The prediction results showed that compound **128** had a high unbound fraction, which amounted to 84.737%. This indicates that the majority of this compound is available in free form to interact with biological targets. This increases its therapeutic potential as more compounds are available to exert pharmacological effects. In terms of metabolism, compound **128** is a substrate for several CYP450 enzymes, namely CYP1A2, CYP2C9, and CYP2D6, but does not inhibit these enzymes. This suggests that this compound will be metabolized by these enzymes in the liver. In the human liver, CYP2C9 stands out as a major enzyme in the CYP2C subfamily, playing an important role in metabolizing clinically relevant drugs with a narrow therapeutic range.<sup>68</sup>

Drug excretion encompasses a range of processes that eliminate a specific drug and/or its metabolites from the body. It represents the ultimate stage in the ADME (Absorption, Distribution, Metabolism, and Excretion) process. Excreted drugs may be re-mobilized in an unmetabolized form or eliminated after metabolic biotransformation.<sup>69</sup> Drug excretion parameters evaluated *in silico* include drug clearance and half-life ( $t_{1/2}$ ). Drug clearance refers to the amount of medications clear from the plasma in the vascular compartment within a specific time period. Total clearance is a measure of drug removal from the central compartment, independent of the specific mechanism involved in this process. Based on the ADMETlab model prediction, a drug is classified as having high clearance if its expected value exceeds 15 mL/min/kg, moderate clearance if the predicted value falls between 5 and 15 mL/min/kg, and low clearance if it is less than 5 mL/min/kg.<sup>30</sup> Alkaloid compound **128** is predicted to have moderate clearance, with a value of 3090 mL/min/kg. Moderate clearance indicates that compound **128** is eliminated from the body at a moderate rate. This means that the drug is not eliminated from the body too quickly, so therapeutic concentrations can be maintained without the need for very frequent dosing, and the risk of drug accumulation that can cause toxicity is also lower.

Based on Lipinski's Rule of Five, compound **128** shows favorable characteristics for being developed as an oral drug. Compound **128** fulfills all Lipinski's Ro5 criteria, ie, molecular weight less than 500 g/mol, ie, 246.30 g/mol, number of hydrogen bond donors not more than 5, ie, only 1 bond, number of hydrogen bond acceptors not more than 10, ie, only 2 bonds, and all log P values not more than 5. Compliance with physicochemical criteria and pharmacokinetic data

supports the potential of this compound to have good bioavailability and a low risk of drug interactions. It can be used for further development, and research and clinical trials are needed to confirm the effectiveness and safety of this compound as a good drug candidate.

## Conclusion

This study successfully identified alkaloids from the genus *Erythrina* that have potential as AChE inhibitors. Compound 8-oxoerymelanthine (**128**) is a potential strong candidate with low toxicity profile and good pharmacokinetic properties, making it worthy of further research in the development of AD therapy. Through in silico studies with a combination of molecular docking, pharmacokinetic studies, toxicity, and Ro5 calculations, and molecular dynamics simulations, compound **128** was evaluated to have potential as an AChE inhibitor. This compound is a promising candidate for further investigation and development as an inhibitory agent, and deserves consideration as a potential component for the development of new drug compounds.

Compound 128 exhibits significant binding affinity and stability towards AChE through interactions akin to galantamine, albeit with notable distinctions. The RMSF analysis indicates that the stability of the AChE catalytic domain, encompassing critical residues such as TRP86, TYR337, TYR133, HIE447, GLU202, and SER203, exhibits minimal fluctuations. This stability underpins the efficacy of the catalytic reaction and ligand binding, suggesting that AChE maintains stability in the transition state, which is crucial for preventing interruptions in the catalytic process. Compound 128 engages with critical residues including TRP, TYR, HIE, SER, GLY, and GLU, establishing conventional hydrogen bonds and stable pi-alkyl interactions, akin to the binding mechanism of galantamine. The enhanced pi-pi-stacked interactions between compound 128 and AChE suggest that this molecule may effectively emulate galantamine binding, resulting in powerful AChE inhibition.

Compound 128 possesses a greater number of aromatic rings, facilitating enhanced and more robust Pi-Pi interactions, particularly in the form of stacked Pi-Pi interactions, which exhibit increased stability. The enhanced flexibility allows compound 128 to more effectively conform to the AChE active site, resulting in increased non-covalent interactions and improved binding affinity. This chemical process elucidates how compound 128 enhances its affinity for AChE, suggesting the potential for more potent and selective enzyme inhibition. While galantamine is beneficial for Alzheimer's treatment, compound 128 may serve as a more efficient and enduring option due to its capacity to establish stronger non-covalent connections. Consequently, compound 128 presents a greater possibility for elevating acetylcholine levels and delivering more efficacious treatment for Alzheimer's patients. Further study of alkaloids from the genus *Erythrina* may provide promising results in the field of neurodegenerative disease research. However, additional exploration and research is required to validate the inhibitory compounds through experimental procedures in vitro and advance them to pre-clinical and clinical studies. This aims to enable the assessment of the safety and efficacy of *Erythrina* alkaloid compounds as potential therapeutic agents.

## Ethics Statement

This study does not include human data or human and animal subjects. The research was conducted exclusively using in silico analysis.

## Acknowledgments

The authors are grateful for the facilities from Universitas Padjadjaran (Indonesia), Scholarship from Kemenkeu, and Kemendikbudristek that have funded this research, Master Thesis Research, with grant numbers (038/E5/PG.02.00.PM/2023 and 3019/UN6.3.1/PM.00/2023) and also express our gratitude to Lembaga Pengelola Dana Pendidikan (LPDP) for its support in the publication of this article.

## Disclosure

The authors report no conflicts of interest in this work.



## References

1. Tiwari S, Atluri V, Kaushik A, et al. Alzheimer's disease: pathogenesis, diagnostics, and therapeutics. *Int J Nanomed*. 2019;14:5541–5554. doi:10.2147/IJN.S200490
2. Subramanian A, Tamilanban T, Alsayari A, et al. Trilateral association of autophagy, mTOR and Alzheimer's disease: potential pathway in the development for Alzheimer's disease therapy. *Front Pharmacol*. 2022;13:1094351. doi:10.3389/fphar.2022.1094351
3. Reshma A, Subramanian A, Kumarasamy V, et al. Neurocognitive effects of proanthocyanidin in Alzheimer's disease: a systematic review of preclinical evidence. *Braz J Med Biol Res*. 2024;57:e13587. doi:10.1590/1414-431X2024e13587
4. Subramanian A, Taminlaban T, Kumarasamy V, et al. Design, synthesis, and invitro pharmacological evaluation of novel resveratrol surrogate molecules against Alzheimer's disease. *Chem Biodivers*. 2024;21(9):e202401430. doi:10.1002/cbdv.202401430
5. Giacobini E. Cholinesterases: new roles in brain function and in Alzheimer's disease. *Neurochem Res*. 2003;21(9):e202401430. doi:10.1002/cbdv.202401430
6. Anawal ML, Chandakavate S, Lalitha S, et al. A comprehensive review on Alzheimer's disease. *World J Pharm Pharm Sci*. 2021;10:1170–1185. doi:10.20959/wjpps20217-19427
7. Subramanian A, Tamilanban T, Subramaniyan V, et al. Establishing network pharmacology between natural polyphenols and Alzheimer's disease using bioinformatic tools – an advancement in Alzheimer's research. *Toxicol Rep*. 2024;13:101715. doi:10.1016/j.toxrep.2024.101715
8. Sarkar B, Alam S, Rajib TK, et al. Identification of the most potent acetylcholinesterase inhibitors from plants for possible treatment of Alzheimer's disease: a computational approach. *Egypt J Med Hum Genet*. 2021;22(10). doi:10.1186/s43042-020-00127-8
9. Hampel H, Mesulam MM, Cuello AC, et al. Revisiting the cholinergic hypothesis in Alzheimer's disease: emerging evidence from translational and clinical research. *J Prev Alzheimers Dis*. 2019;6(1):2–15. doi:10.14283/jpad.2018.43
10. Hampel H, Mesulam MM, Cuello AC, et al. The cholinergic system in the pathophysiology and treatment of Alzheimer's disease. *Brain*. 2018;141(7):1917–1933. doi:10.1093/brain/awy132
11. Asgharian P, Quispe C, Harrera-Bravo J, et al. Pharmacological effects and therapeutic potential of natural compounds in neuropsychiatric disorders: an update. *Front Pharmacol*. 2022;13:926607. doi:10.3389/fphar.2022.926607
12. Van NV. The use of medicinal plants as immunostimulants in aquaculture: a review. *Aquaculture*. 2015;446:88–96. doi:10.1016/j.aquaculture.2015.03.014
13. Konrath EL, Passos Cdos S, Klein LC Jr, et al. Alkaloids as a source of potential anticholinesterase inhibitors for the treatment of Alzheimer's disease. *J Pharm Pharmacol*. 2013;65(12):1701–1725. doi:10.1111/jphp.12090
14. Dos Santos TC, Gomes TM, Pinto BAS, et al. Naturally occurring acetylcholinesterase inhibitors and their potential use for Alzheimer's disease therapy. *Front Pharmacol*. 2018;9:1–14. doi:10.3389/fphar.2018.01192
15. Bourne Y, Taylor P, Radić Z, et al. Structural insights into ligand interactions at the acetylcholinesterase peripheral anionic site. *EMBO J*. 2003;22(1):1–12. doi:10.1093/emboj/cdg005
16. Kikuchi T, Okamura T, Fukushi K, et al. Cerebral acetylcholinesterase imaging: development of the radioprobes. *Curr Top Med Chem*. 2007;7(18):1790–1799. doi:10.2174/156802607782507466
17. Zhou B, Zhang B, Li X, et al. New 2-Aryl-9-methyl- $\beta$ -carbolinium salts as potential acetylcholinesterase inhibitor agents: synthesis, bioactivity and structure-activity relationship. *Sci Rep*. 2018;8(1):1559. doi:10.1038/s41598-018-19999-3
18. Zhao Q, Yang G, Mei X, et al. Design of novel carbamate acetylcholinesterase inhibitors based on the multiple binding sites of acetylcholinesterase. *J Pestic Sci*. 2008;33(4):371–375. doi:10.1584/jpestics.G08-25
19. Piazzi L, Cavalli A, Belluti F, et al. Extensive SAR and computational studies of 3-{4-[(Benzylmethylamino)methyl]phenyl}-6,7-dimethoxy-2H-2-chromenone (AP2238) Derivatives. *J Med Chem*. 2007;50(17):4250–4254. doi:10.1021/jm070100g
20. Lushchekina SV, Makhaeva GF, Novichkova DA, et al. Supercomputer modeling of dual-site acetylcholinesterase (AChE) inhibition. *Supercomput Front Innov*. 2008;5:89–97. doi:10.14529/jsfi180410
21. Fahmy NM, Al-Sayed E, El-Shazly M, et al. Alkaloids of genus Erythrina: an updated review. *Nat Prod Res*. 2020;34(13):1891–1912. doi:10.1080/14786419.2018.1564300
22. Santos WP, Da Silva Carvalho AC, Dos Santos Estevam C, et al. In vitro and ex vivo anticholinesterase activities of *Erythrina velutina* leaf extracts. *Pharm Biol*. 2012;50(7):919–924. doi:10.3109/13880209.2011.649429
23. Patil VS, Meena H, Harish DR. *Erythrina variegata* L. bark: an untapped bioactive source harbouring therapeutic properties for the treatment of Alzheimer's disease. *In Silico Pharmacol*. 2021;9(1):51. doi:10.1007/s40203-021-00110-0
24. Salem A, Mostafa N, Al-Sayed E, et al. Erythrina alkaloids: an updated review with neurological perspective. *Archiv Pharmaceutical Sci Ain Shams Univ*. 2023;7(1):171–199. doi:10.21608/aps.2023.207482.1119
25. Setti-Perdigão P, Serrano MA, Flausino OA Jr, et al. Erythrina mulungu alkaloids are potent inhibitors of neuronal nicotinic receptor currents in mammalian cells. *PLoS One*. 2013;8(12):e82726. doi:10.1371/journal.pone.0082726
26. Dias KCF, de Almeida JC, Vasconcelos LC, et al. Standardized extract of *Erythrina velutina* Willd. attenuates schizophrenia-Like behaviours and oxidative parameters in experimental animal models. *J Pharm Pharmacol*. 2019;71(3):379–389. doi:10.1111/jphp.13039
27. Patel P, Noyda I, Kagathara M, et al. Alzheimer's disease: the review from pathophysiology to future direction. *Technoarete Transact Recent Res Appl Microbiol Biotechnol*. 2023;2(1):6–12. doi:10.36647/TTRRAMB/02.01.A002
28. Forli S, Huey R, Pique ME, et al. Computational protein-ligand docking and virtual drug screening with the AutoDock suite. *J Nat Protoc*. 2016;11(5):905–919. doi:10.1038/nprot.2016.051
29. Cheung J, Rudolph MJ, Burshteyn F, et al. Structures of human acetylcholinesterase in complex with pharmacologically important ligands. *J Med Chem*. 2012;55(22):10282–10286. doi:10.1021/jm300871x
30. Pires DEV, Blundell TL, Ascher DB, et al. pkCSM: predicting small-molecule pharmacokinetic and toxicity properties using graph-based signatures. *J Med Chem*. 2015;58(9):4066–4072. doi:10.1021/acs.jmedchem.5b00104
31. Cheng F, Li W, Zhou Y, et al. admetSAR: a comprehensive source and free tool for assessment of chemical ADMET properties. *J Chem Inf Model*. 2012;52(11):3099–3105. doi:10.1021/ci300367a
32. Lipinski CA, Lombardo F, Dominy BW, et al. Experimental and computational approaches to estimate solubility and permeability in drug discovery and development settings. *J Adv Drug Deliv Rev*. 2012;64:4–17. doi:10.1016/j.addr.2012.09.019

33. Hardianto A, Mardetia SS, Destiarani W, et al. Unveiling the anti-cancer potential of onoceranoid triterpenes from *Lansium domesticum* corr. cv. kokosan: an in silico study against estrogen receptor alpha. *Int J mol Sci.* **2023**;24(19):15033. doi:10.3390/ijms241915033
34. Hardianto A, Yusuf M, Hidayat IW, et al. Exploring the potency of *Nigella sativa* seed in inhibiting SARS-CoV-2 main protease using molecular docking and molecular dynamics simulations. *Indonesian J Chem.* **2021**;21(5):1252–1262. doi:10.22146/ijc.65951
35. Herlina T, Akili AWR, Nishinarizki V, et al. Cytotoxic evaluation, molecular docking, molecular dynamics, and ADMET Prediction of Isolupalbigenin Isolated from *Erythrina subumbrans* (hassk). merr. (fabaceae) stem bark: unveiling its anticancer efficacy. *Onco Targets Ther.* **2024**;17:829–840. doi:10.2147/OTT.S482469
36. Gupta R, Polaka S, Rajpoot K, et al. Importance of toxicity testing in drug discovery and research. *Pharmacokinetics and Toxicokinetic Considerations.* **2022**;2. doi:10.1016/b978-0-323-98367-9.00016-0.
37. Vedani A, Smiesko M. In silico toxicology in drug discovery - concepts based on three-dimensional mod-els. *Altern Lab Anim.* **2009**;37(5):477–496. doi:10.1177/026119290903700506
38. Azam F, Taban IM, Eid EEM, et al. An in-silico analysis of ivermectin interaction with potential SARS-CoV-2 targets and host nuclear importin  $\alpha$ . *J Biomol Struct Dyn.* **2022**;40(6):2851–2864. doi:10.1080/07391102.2020.1841028
39. Lillis D. Use R for data analysis and research. *New Zealand Science Review.* **2023**;68(2):73–79. doi:10.26686/nzsr.v68.8841
40. Raj R. Analysis of non-structural proteins, NSPs of SARS-CoV-2 as targets for computational drug designing. *Biochem Biophys Rep.* **2021**;25:100847. doi:10.1016/j.bbrep.2020.100847
41. Iqbal D, Rehman MT, Bin Dukhyil A, et al. High-throughput screening and molecular dynamics simulation of natural product-like compounds against alzheimer's disease through multitarget approach. *Pharmaceuticals (Basel).* **2021**;14(9):1–19. doi:10.3390/ph14090937
42. Okocha RC, Olatoye IO, Adedeji OB. Food safety impacts of antimicrobial use and their residues in aquaculture. *Public Health Rev.* **2018**;39(1):1–22. doi:10.1186/s40985-018-0099-2
43. Meunier L, Larrey D. Drug-induced liver injury: biomarkers, requirements, candidates, and validation. *Front Pharmacol.* **2019**;10:1–8. doi:10.3389/fphar.2019.01482
44. Pitera JW. Expected distributions of root-mean-square positional deviations in proteins. *J Phys Chem B.* **2014**;118(24):6526–6530. doi:10.1021/jp412776d
45. Nishinarizki V, Hardianto A, Gaffar S, et al. Virtual screening campaigns and ADMET evaluation to unlock the potency of flavonoids from *Erythrina* as 3CLpro SARS-COV-2 inhibitors. *J Appl Pharm Sci.* **2023**;13:78–88. doi:10.7324/japs.2023.130209
46. Kuzmanic A, Zagrovic B. Determination of ensemble-average pairwise root mean-square deviation from experimental B-factors. *Biophysj.* **2010**;98(5):861–871. doi:10.1016/j.bpj.2009.11.011
47. Ghahremanian S, Rashidi MM, Raeisi K, et al. Molecular dynamics simulation approach for discovering potential inhibitors against SARS-CoV-2: a structural review. *J Mol Liq.* **2022**;354. doi:10.1016/j.molliq.2022.118901.
48. Cob-Calan NN, Chi-Uluac LA, Ortiz-Chi F, et al. Molecular docking and dynamics simulation of protein  $\beta$ -tubulin and antifungal cyclic lipopeptides. *Molecules.* **2019**;24(18):3387. doi:10.3390/molecules24183387
49. Tripathi N, Goel B, Bhardwaj N, et al. Virtual screening and molecular simulation study of natural products database for lead identification of novel coronavirus main protease inhibitors. *J Biomol Struct Dyn.* **2022**;40(8):3655–3667. doi:10.1080/07391102.2020.1848630
50. Silman I, Sussman JL. Acetylcholinesterase: how is structure related to function? *Chem Biol Interact.* **2008**;175(1–3):3–10. doi:10.1016/j.cbi.2008.05.035
51. Macdonald IR, Martin E, Rosenberry TL, et al. Probing the peripheral site of human butyrylcholinesterase. *Biochemistry.* **2012**;51(36):7046–7053. doi:10.1021/bi300955k
52. Liu Z, Fu X, Yuan M, et al. International journal of biological macromolecules surface charged amino acid-based strategy for rational engineering of kinetic stability and specific activity of enzymes: linking experiments with computational modeling. *Int J Biol Macromol.* **2021**;182:228–236. doi:10.1016/j.ijbiomac.2021.03.198
53. Zhang Y, Kua J, McCommon JA. Role of the catalytic triad and oxyanion hole in acetylcholinesterase catalysis: an ab initio QM/MM Study. *J Am Chem Soc.* **2002**;124(35):10572–10577. doi:10.1021/ja020243m
54. Gao D, Zhan CG. Modeling effects of oxyanion hole on the ester hydrolysis catalyzed by human cholinesterases. *J Phys Chem B.* **2005**;109(48):23070–23076. doi:10.1021/jp053736x
55. Shi J, Tai K, McCommon JA, et al. Nanosecond dynamics of the mouse acetylcholinesterase cys 69 – cys 96 omega loop \*. *J Biol Chem.* **2003**;278(33):30905–30911. doi:10.1074/jbc.M303730200
56. Bui JM, Henchman RH, McCommon JA. The dynamics of ligand barrier crossing inside the acetylcholinesterase gorge. *Biophys. J.* **2003**;85(4):2267–2272. doi:10.1016/s0006-3495(03)74651-7
57. Choudhary MI, Nawaz SA, Zaheer U-H, et al. Juliflorine: a potent natural peripheral anionic-site-binding inhibitor of acetylcholinesterase with calcium-channel blocking potential, a leading candidate for Alzheimer's disease therapy. *Biochem Biophys Res Commun.* **2005**;332(4):1171–1177. doi:10.1016/j.bbrc.2005.05.068
58. Zhu Y, Alqahtani S, Hu X. Aromatic rings as molecular determinants for the molecular recognition of protein kinase inhibitors. *Molecules.* **2021**;26(6):1–18. doi:10.3390/molecules26061776
59. Son NT, Elshamy AI. Flavonoids and other non-alkaloidal constituents of genus *Erythrina*: phytochemical Review. *Comb Chem High Throughput Screen.* **2021**;24(1):20–58. doi:10.2174/1386207323666200609141517
60. Plaper A, Golob M, Hafner I, et al. Characterization of quercetin binding site on DNA gyrase. *Biochem Biophys Res Commun.* **2023**;306(2):530–536. doi:10.1016/S0006-291X(03)01006-4
61. Schaduagratt N, Lampa S, Simeon S, et al. Towards reproducible computational drug discovery. *J Cheminform.* **2020**;12(1):9. doi:10.1186/s13321-020-0408-x
62. Bittermann K, Goss KU. Predicting apparent passive permeability of Caco-2 and MDCK cell-monolayers: a mechanistic model. *PLoS One.* **2017**;12(12):e0190319. doi:10.1371/journal.pone.0190319
63. Trejo-Lopez JA, Yachnis A, Prokop S, et al. Neuropathology of Alzheimer's disease. *Neurotherapeutics.* **2022**;19(1):173–185. doi:10.1007/s13311-021-01146-y
64. Á L-B, Garza-Cárdenas C, Garza-Cervantes J, et al. The demand for new antibiotics: antimicrobial peptides, nanoparticles, and combinatorial therapies as future strategies in antibacterial agent design. *Front Microbiol.* **2020**;11:1669. doi:10.3389/fmicb.2020.01669

65. Lahlou M. Screening of natural products for drug discovery. *Expert Opin Drug Discov.* 2007;2(5):697–705. doi:10.1517/17460441.2.5.697
66. Akili AWR, Hardianto A, Latip J, et al. Virtual Screening and ADMET Prediction to Uncover the Potency of Flavonoids from Genus *Erythrina* as Antibacterial Agent through Inhibition of Bacterial ATPase DNA Gyrase B. *Molecules.* 2023;28(24):8010. doi:10.3390/molecules28248010
67. Bernardo-castro S, Sousa JA, Brás A, et al. Pathophysiology of Blood – brain Barrier Permeability Throughout the Different Stages of Ischemic Stroke and Its Implication on Hemorrhagic Transformation and Recovery. *Front Neurol.* 2020;11:1–24. doi:10.3389/fneur.2020.594672
68. Daly AK, Rettie AE, Fowler DM, et al. Pharmacogenomics of CYP2C9: functional and clinical considerations. *J Pers Med.* 2018;8(1):1–31. doi:10.3390/jpm8010001
69. Currie GM. Pharmacology, Part 2: introduction to Pharmacokinetics. *J Nucl Med Technol.* 2021;221–230. doi:10.2967/jnmt.117.199638

## Advances and Applications in Bioinformatics and Chemistry

**Dovepress**  
Taylor & Francis Group

### Publish your work in this journal

Advances and Applications in Bioinformatics and Chemistry is an international, peer-reviewed open-access journal that publishes articles in the following fields: Computational biomodelling; Bioinformatics; Computational genomics; Molecular modelling; Protein structure modelling and structural genomics; Systems Biology; Computational Biochemistry; Computational Biophysics; Chemoinformatics and Drug Design; In silico ADME/Tox prediction. The manuscript management system is completely online and includes a very quick and fair peer-review system, which is all easy to use. Visit <http://www.dovepress.com/testimonials.php> to read real quotes from published authors.

Submit your manuscript here: <https://www.dovepress.com/advances-and-applications-in-bioinformatics-and-chemistry-journal>